SLAC-PUB-17326
September 17, 2022

Kinetic Mixing and Portal Matter Phenomenology

Thomas G. Rizzo †

SLAC National Accelerator Laboratory 2575 Sand Hill Rd., Menlo Park, CA, 94025 USA

arXiv:1810.07531v1 [hep-ph] 17 Oct 2018

Abstract

Dark photons (DP) are interesting as potential mediators between the dark matter (DM) sector and the fields of the Standard Model (SM). The interaction of the DP, described by a broken $U(1)_D$ gauge symmetry, with the SM is usually generated at the one-loop level via kinetic mixing through the existence of portal matter (PM), here assumed to be fermionic, which carries both a dark charge as well as a SM $U(1)_Y$ hypercharge. For theoretical consistency, as well as for many phenomenological reasons, this PM must be vector-like with respect to the SM and dark gauge groups and, in particular, is shown to be allowed only to transform as vector-like copies of the usual SM fields. The dark Higgs that is responsible for the breaking of $U(1)_D$ can then generate a mixing between the PM and SM fields with the same electric charge thus altering the DP interactions with (at least some of) the SM fields and also providing a path for the PM fields to decay. In this paper we briefly explore the phenomenology of some specific simple models of this PM including, for the case where the PM is leptonic in nature, their potential impact on experiments probing low energy parity-violation and the g-2 of the muon. In the case of color-triplet, bottom quark-like PM, their direct pair- and single-production at the LHC is shown to be observable in final states that include missing E_T and/or very highly boosted lepton-jets together with pairs of high p_T b-jets that can be used to trigger on such events. These signatures are quite distinct from those usually employed in the search for vector-like quarks at the LHC and, furthermore, we demonstrate that the conventional signal channels for vector-like quarks involving the SM Higgs and gauge fields are essentially closed in the case of PM. Many other more complex, and more realistic, PM scenarios of the type discussed here are possible which can lead to wide-ranging signatures in various classes of experiments.

† rizzo@slac.stanford.edu

1 Introduction

The nature of dark matter (DM) remains as one of the great mysteries facing particle physics. For DM to achieve its observed abundance, it is probable that it must have some new, non-gravitational interaction with the fields of the Standard Model (SM) - but such interactions are likely to be far weaker than the usual ones with which we are familiar. Traditionally, both axions [1, 2] and WIMPS [3] have been the leading candidates for DM, originating in top-down frameworks that addressed other issues such as the strong CP problem and naturalness. Searches for such particles have so far obtained only null results and while these important experiments are still evolving the set of possible DM candidates continues to grow as does the possible ways to look for them [4, 5]. Among these, one of the most interesting and directly testable possibilities that has garnered much recent attention is the kinetic mixing/vector portal model [6, 7]. In its most simple form, this setup assumes the existence of a dark photon (DP), *i.e.*, the gauge field of a new $U(1)_D$, that is spontaneously broken through the vacuum expectation value (vev) of a complex SM singlet dark Higgs, $< S >= v_s/\sqrt{2}$, with $v_s \sim 0.1$ to a few GeV. The DM field carries a non-zero dark charge, Q_D, so that it can couple directly to the DP. On the other hand, the SM fields do not carry any dark charges under this $U(1)_D$ so that the interactions of the DP with the SM fields are loop-induced via the kinetic mixing (KM) of the DP with the usual SM $U(1)_Y$ hypercharge field, B_μ, whose strength is characterized by a parameter $\epsilon \sim 10^{-(3-5)}$. The vacuum polarization-like diagram that generates this interaction is the result of the existence of an important (though much neglected) new set of fields which carry *both* SM as well as dark charges and we will refer to such dually-charged states as portal matter (PM) in what follows. This PM plays an essential role in all models where the DM interactions with the SM are induced by KM. To obtain a non-zero and yet finite result, several, non-degenerate PM fields are required, the product of whose charges must satisfy the condition $\sum_i Q_{Y_i} Q_{D_i} = 0$. What are these PM states and how do they impact non-DM phenomenology? It is the nature of these PM fields, their interactions with the DP, as well as with the familiar SM particles that will be of interest to us below.

If the PM fields are fermionic, which we will argue below is the most likely scenario and which we will assume in the following discussion, they must be vector-like with respect to both the $U(1)_D$ and the SM gauge groups in order to avoid various gauge anomalies, precision electroweak constraints and the additional constraints coming from Higgs boson production via gg fusion at the LHC. Such vector-like fermions (VLF) are then qualitatively similar in nature to those that have been well-studied in various extensions of the SM [8] and which have been sought at the LHC without success (so far) by both the ATLAS and CMS collaborations [9]. The difference in the present case is that these PM fields also carry dark charges so that they cannot mix with the correspondingly charged SM fields via a Yukawa coupling with the SM Higgs. This implies that their decays to final states involving either the SM Higgs or SM gauge bosons are highly suppressed yet these are the modes being searched for at the LHC. However, such mixings between the PM and the fermion fields of the SM can occur when the $U(1)_D$ charges of these PM fields allow for an analogous Yukawa coupling to the *dark* Higgs which, as we'll see below, leads to quite a different phenomenology and production signatures at the LHC now involving long-lived states arising from the DP and dark Higgs. As we will discuss, the existence of such states can also have direct impact on other experiments performed at lower energies depending upon their specific SM quantum numbers.

The outline of this paper is as follows: Section 2 begins by providing a general overview of the KM/DP setup and the role that PM plays within it. After specializing to the case of the PM being a set of SM-like VLF, the mixing of these PM fields with those of the SM are analyzed in detail in the most minimal scenario involving only a single flavor pair of PM fields. Section 3 provides a non-comprehensive survey of some of the possible phenomenological implication of the existence of the mixing between the SM fields and the PM but which depend on the detailed SM quantum numbers assumed for the PM states. The modifications of the DP couplings to the SM fields that are induced by this mixing are then considered; it is pointed out that these, generally parity-violating, contributions can be comparable in strength to those induced by the familiar KM. The PM/SM mixing also induces off diagonal couplings of these PM/SM fields to both the DP and the dark Higgs. If the PM transforms like a SM right-handed electron then such new parity-violating effects may be observable in low energy experiments such as MOLLER. If the PM is μ_R-like in nature, this leads to multiple new contributions to the g-2 of the muon, whose experimental

value is known to differ from the SM prediction by $\sim 4\sigma$. We note that if the PM were similar to the left-handed lepton doublet, then the mixing with the VLF N induces a new low-Q^2 interaction between neutrinos and quarks which may impact measurements at, *e.g.*, MiniBooNE. Lastly, and in more detail, we consider the setup where the PM transforms like b_R in the SM; in such a case a variety of possible signals can arise from their pair production at the LHC. In addition to the two, high-p_T, b-jets produced in PM pair decay, the final state is shown to include missing E_T, producing a SUSY-like signature, and/or displaced lepton-jets which are atypical due their very large boosts. The case where the b_R-like PM is singly produced is also briefly discussed and shown to lead to asymmetrically boosted lepton-jets. Section 4 contains a final discussion and our conclusions.

2 Portal Matter Phenomenology Setup

Consider a set of VLF with masses m_i and whose hypercharges and corresponding dark charges are denoted by Q_{Y_i} and Q_{D_i}, respectively. Then, in conventional normalization, the familiar 1-loop vacuum polarization-like graph coupling the two corresponding gauge fields will lead to a KM parameter $\epsilon \sim 10^{-(3-5)}$ given by ($c_W = \cos\theta_W$)

$$\epsilon = c_W \frac{g_D g_Y}{12\pi^2} \sum_i \; Q_{Y_i} Q_{D_i} \; ln \frac{m_i^2}{\mu^2} \tag{1}$$

where a finite result requires that these fields be non-degenerate and satisfy the constraint $\sum_i Q_{Y_i} Q_{D_i} = 0$ and where $g_{Y,D}$ are the hypercharge and dark gauge coupling constants, respectively. We will assume that $g_D \sim 0.1 - 0.3$ in our numerical analysis that follows. The simplest possibility, which we will consider here, is thus where there are only two such VLF, $F_{1,2}$, with different masses, having the same value of the SM hypercharge but with simultaneously opposite values for Q_D; we will take this numerical value to be unity, $|Q_{D_i}| = 1$, without loss of generality in the present analysis. Thus, in this limited discussion, we will constrain ourselves to the case where the PM consists of a single pair of fields that have identical SM characteristics. (Clearly, we can generalize far beyond this simplifying assumption to more complex situations but we will leave this to later work.) Given these considerations, we then obtain numerically

$$\epsilon \simeq 1.0 \Big(\frac{g_D}{0.1}\Big) N_c Q_Y \frac{ln(m_2/m_1)}{ln\ 1.5} \cdot 10^{-4} \tag{2}$$

a value which is consistent with our expectations and where N_c is the number of colors of the PM fields. Since these PM states carry both SM and dark charges they must be unstable and a decay path for them must be generated in any realistic theory. In practice this implies that they must mix with the analogous SM fields as we will discuss further below. It should be stressed that this simple scenario need not be the one that is actually realized in nature. For example, one can imagine, *e.g.*, MP contributions from color triplet, weak iso-singlets 'canceling' against those from color singlet, weak iso-doublets as in a $5 + \bar{5}$ SU(5)-like representation. Such possibilities will be considered elsewhere but one should be mindful of their potential phenomenological impact which may simultaneously lie in multiple sectors. We note in passing that if we had chosen the PM to be complex scalars *without* vevs, it is much more difficult to arrange for them to decay via mixing with the analogous SM field, *i.e.*, the Higgs, which is the only available SM scalar, without further augmentation of the model.

Once a value of $\epsilon \neq 0$ is obtained this leads to the now standard development via the Lagrangian

$$\mathcal{L} = \mathcal{L}_1 + \mathcal{L}_2 + \mathcal{L}_{HS} + \mathcal{L}_{Portal} \tag{3}$$

with the $\mathcal{L}_1$ piece of the action describing the DP field, $\hat{V}$, the corresponding hypercharge gauge field, $\hat{B}$, and the rest of the SM:

$$\mathcal{L}_1 = \; -\frac{1}{4}\hat{V}_{\mu\nu}\hat{V}^{\mu\nu} - \frac{1}{4}\hat{B}_{\mu\nu}\hat{B}^{\mu\nu} + \frac{\epsilon}{2c_w}\hat{V}_{\mu\nu}\hat{B}^{\mu\nu} + \mathcal{L}_{SM}\,, \tag{4}$$

and, with $D_\mu = \partial_\mu + ig_D Q_D \hat{V}_\mu$ being the gauge covariant derivative in obvious notation,

$$\mathcal{L}_2 = \; i\bar{\chi}\gamma^\mu D_\mu \chi - m_D \bar{\chi}\chi + (D_\mu S)^\dagger (D^\mu S) + \mu_S^2 S^\dagger S - \lambda_S (S^\dagger S)^2 \,, \tag{5}$$

which describes the DM field χ[1]. Note that here the DM is assumed to be a fermion (which does not couple directly to the SM) for definiteness but the detailed nature of the DM will not play a large role in the discussion below. This same piece of the action also describes the dark Higgs, S[2]. We will make the further assumption in our discussion below that $2m_D > m_V$ such that V must decay to SM fields, *e.g.*, e^+e^-, so that this state may be observable at, *e.g.*, HPS [11] and not at, *e.g.*, LDMX [12] if one searches only for final states with missing energy/momentum. The KM in $\mathcal{L}_1$ is removed and the fields become canonically normalized via the field re-definitions (to lowest order in ϵ), $\hat{B}_\nu \to B_\nu + \frac{\epsilon}{c_W} V_\nu$, $\hat{V}_\nu \to V_\nu$. After this transformation and mass mixing with the SM Z generated via the vev of the SM Higgs, H, is accounted for (in the limit of small m_V^2/m_Z^2 as is relevant in the present case), the physical V mass eigenstate couples to the SM fields as $\simeq e\epsilon Q_{em}$. It should be noted that since $m_V = g_D v_s$ with $g_D \sim 0.1 - 0.3$ being assumed here while S has a mass $\sqrt{2\lambda_S} v_s$ it is natural that $m_S > m_V$ since g_D is small. Note that S has no gauge-invariant, renormalizable coupling to the Dirac fermion DM. This implies that, in the absence of mixing with the SM Higgs, S decays as $S \to VV^*, V^* \to e^+e^-$ and possibly more likely via the on-shell process $S \to VV$ and not directly to DM states. In the $S \to VV$ case, this decay is prompt as $g_D \sim 0.1 - 0.3$; this will be important in the discussion that follows.

As usual the H and S Higgs fields can also mix due to their vevs through the standard quartic term

$$\mathcal{L}_{HS} = \; \lambda_{HS} H^\dagger H S^\dagger S \tag{6}$$

with the magnitude of λ_{HS} usually and necessarily being fine-tuned to very small values (unlike what can happen by employing extra dimensions [13, 14] where this mixing can be set to zero via a choice of boundary conditions) to meet phenomenological constraints arising from measurements of Higgs properties at the LHC. To get an idea of this stringent requirement which will be important in later discussions, we can compare the mixing-induced partial width $\Gamma(H \to SS + VV)$ to the present limit on the invisible Higgs branching fraction $B = BF(H \to inv) \lesssim 0.2$. To leading order in this mixing, the HSS coupling is just $\simeq \lambda_{HS}/2\lambda_H$ with $\lambda_H \simeq 0.129$ since $m_H \simeq 125$ GeV. Some algebra then tells us that this BF bound implies that $|\lambda_{HS}| \lesssim 4.7 \cdot 10^{-3} \sqrt{B/0.1}$. Since one finds that the $H - S$ mixing angle is then $\theta_{HS} \simeq -\lambda_{HS} v_s / 2\lambda_H v_H$, this result further implies that $|\theta_{HS}| \lesssim 1.8 \cdot 10^{-4} \left(\frac{v_s/v_H}{10^{-2}}\right) \sqrt{B/0.1}$. Here, except where noted, we will generally set the λ_{HS} coupling to an extremely small value, corresponding to a very tight mixing angle bound, so that its influence on the dark sector fields can generally be safely ignored. However, we will return to this very important point later on.

So far we have briefly summarized the usual development of the DP/KM scenario to establish notation and basic assumptions; now let us return to a discussion of the PM part of the action. We recall that these PM states must be unstable so that at least one path for their decay must exist. For the more 'conventional' VLF that are usually discussed such paths are provided by their mixing (via the vev of the SM Higgs) with the analogous SM states which carry the same QCD and QED quantum numbers. For MP states this mixing option does not occur as they also carry dark charges while the SM Higgs does not and so a gauge-invariant coupling of the required type is absent. We can, however, arrange something quite similar employing instead the SM singlet dark Higgs. Amongst the many *a priori* possibilities to consider at the renormalizable level, since the dark Higgs is a SM singlet, the pair of PM fields, $F_{1,2}$ (with $Q_D = \pm 1$) *must* be chosen to transform as one of the familiar set of vector-like fermions (VLF), either vector-like quarks (VLQ) or vector-like leptons (VLL), which are analogous to the representations appearing in the SM:

$$(T, B)^T, \; (N, E)^T, \; T, \; B, \; E \tag{7}$$

where the simplest (but not necessary) possibility is clearly that the PM are simply one of the $SU(2)_W$ isosinglets, *i.e.*, T, B, E. It is now easy to see that only these 5 particular choices allow for the new states

[1] Additional terms may also be present to generate an additional Majorana mass term for χ if required.

[2] Here we will often write S as $(v_s + S + iG)/\sqrt{2}$, where G is the eaten Goldstone boson and S now represents the remaining real scalar field.

to decay to SM fields at tree-level since S is a SM singlet. To determine how this specific mixing may be generated we imagine that $|Q_D(S)| = 1$; then we can write a new gauge invariant term in the Lagrangian given by

$$\mathcal{L}_{Portal} = \lambda_{1a}\bar{F}_{1L}f^a_R S + \lambda_{2a}\bar{F}_{2L}f^a_R S^\dagger + h.c. \tag{8}$$

with $L(R)$ the usual helicity projections and f^a being the corresponding SM fermion of the same color and hypercharge(*i.e.*, electric charge) with family label $a = 1, 2, 3$. When S gets a vev, this piece of the action will generate off-diagonal mass terms, symbolically of the form $X^a_i = \lambda^a_i v_s/\sqrt{2}$, inducing a mixing between PM fields $F_{1,2}$ with those in the SM, f^a, and eventually between themselves. For simplicity of presentation, we again consider the most simple case where the mixing of the F_i is dominantly with only one generation of the $f^a = f$ which, in the SM, obtains a mass from the usual Higgs mechanism, m_f. Such a possibility can be arranged, *e.g.*, through the proper use of some flavor-dependent discrete symmetries as shown in Ref. [10]. Denoting this set of fermion fields in the original weak basis as $\mathcal{F}^{0T} = (f^0, F^0_1, F^0_2)^T$, the general form of the mass term for these fermions can be written as $\bar{\mathcal{F}}^0_L\mathcal{M}\mathcal{F}^0_R + h.c.$ where

$$\mathcal{M} = \begin{pmatrix} m_f & 0 & 0 \\ X_1 & m_1 & 0 \\ X_2 & 0 & m_2 \end{pmatrix}, \tag{9}$$

which can be diagonalized, as usual, via a bi-unitary transformation $M_D = U_L\mathcal{M}U^\dagger_R$, where M_D is diagonal so that $\mathcal{F}_{L,R} = U_{L,R}\mathcal{F}^0_{L,R}$ are the mass eigenstates. Again, as usual, U_L is determined via the relation $M^2_D = U_L\mathcal{M}\mathcal{M}^\dagger U^\dagger_L$ while U_R is similarly determined via $M^2_D = U_R\mathcal{M}^\dagger\mathcal{M}U^\dagger_R$.

Before proceeding we should say a few words about the values of the entries in $\mathcal{M}$ (outside of the familiar m_f). As we will discuss in more detail below, the PM states $F_{1,2}$ can be pair-produced at the LHC is the same manner as are the more conventional VLF that are usually discussed but which do not carry any dark charges. Thus we might semi-quantitatively expect that $m_{1,2}(T, B) \sim 1 - 2$ TeV while $m_{1,2}(E) \sim 0.3 - 5$ TeV or so based on the current null searches [9] in which only SM particles are involved in the decay. (Of course, as we will stress below, these standard searches for VLF are not applicable in the present case under study.) On the other hand, since v_s is at most a few GeV as we are interested in $m_V = g_D v_s \lesssim 1$ GeV or so, we might then expect that roughly $|X_{1,2}| \sim 1-$a few GeV unless the λ_i are not O(1). With these typical values in mind it is straightforward to determine the matrices $U_{L,R}$ to lowest order in terms of the small set of hierarchal ratios $|X_i|^2/m^2_j$ as

$$U_L = \begin{pmatrix} 1 - m^2_f[X^2_1/(2a^2_1) + X^2_2/(2a^2_2)] & m_f X^*_1/a_1 & m_f X^*_2/a_2 \\ -m_f X_1/a_1 & 1 - m^2_f X^2_1/(2a^2_1) & m^2_2 X_1 X^*_2/(\delta a_1) \\ -m_f X_2/a_2 & -m^2_1 X^*_1 X_2/(\delta a_2) & 1 - m^2_f X^2_2/(2a^2_2) \end{pmatrix}, \tag{10}$$

where we have defined $X^2_i = |X_i|^2$, $a_i = m^2_i - m^2_f$ and $\delta = m^2_1 - m^2_2$; correspondingly, we also obtain

$$U_R = \begin{pmatrix} 1 - [m^2_1 X^2_1/(2a^2_1) + m^2_2 X^2_2/(2a^2_2)] & m_1 X^*_1/a_1 & m_2 X^*_2/a_2 \\ -m_1 X_1/a_1 & 1 - m^2_1 X^2_1/(2a^2_1) & -m_1 m_2 X_1 X^*_2/(\delta a_2) \\ -m_2 X_2/a_2 & m_1 m_2 X^*_1 X_2/(\delta a_1) & 1 - m^2_2 X^2_2/(2a^2_2) \end{pmatrix}. \tag{11}$$

Here we see that, quite generally, the size of the elements in U_R involving the mixing of the VLF with the SM fermion are generally significantly larger than the corresponding ones appearing in U_L. It is interesting to note that if we had instead chosen the PM fermions to be in $SU(2)_W$ doublets we would obtain the same results as above but with the roles of U_L and U_R simply interchanged. We note that in the case of the more 'canonical' iso-singlet VLF that mix with the SM fields via the usual Higgs vev, it is the U_L matrix elements which are large and not the U_R ones as is the case above. Here, since U_L is close to the identity in the present case, as far as any mixing of the PM with the SM fields is concerned, this results in a further suppression of the possible MP decay into the familiar VLF final states involving the SM gauge bosons and Higgs field making these modes essentially irrelevant. The eigenvalues of M^2_D are approximately given to leading order in the mass ratios by $m^2_f(1 + \xi)$ and $m^2_i(1 + \delta_i)$ with $\delta_i \simeq -X^2_i/a_i$

and

$$\xi \simeq -\frac{X_1^2 a_2 + X_2^2 a_1}{a_1 a_2} = \delta_1 + \delta_2 \tag{12}$$

which demonstrates that all of the mass shifts due to mixing are generally fractionally small. Note that all of the expressions above simplify significantly for the cases where $f \neq t$ in which case the m_f^2 terms can always be safely neglected in comparison to the m_i^2. These mixings will allow the PM to decay only to final states which are completely dominated by the presence of V, S.

3 Survey of Phenomenological Implications

Our first goal is to understand how significantly the mixing of the SM fermion, f, with the VLF, F_i, alters its couplings to the DP, both the SM and dark Higgs as well as to the SM gauge bosons. Here we will work in the limit where $m_V^2/m_Z^2 << 1$ so that in the original weak basis the part of the V coupling to the SM due its KM with the hypercharge gauge boson is just $e\epsilon Q_f$ as noted above; note that such a coupling is now experienced by both the usual SM fields as well as by the PM ones since they also carry SM charges. Suppressing Lorentz indices we may express this coupling in the notation above as $e\epsilon Q_f(\bar{\mathcal{F}}_L^0 \mathcal{F}_L^0 + L \to R) \to e\epsilon Q_f(\bar{\mathcal{F}}_L \mathcal{F}_L + L \to R)$ as this part of the interaction is trivially insensitive to the mass mixing of f with $F_{1,2}$. However, we recall that, unlike the SM fields, the PM themselves have a direct coupling to V, $\sim g_D$, even when $\epsilon \to 0$; we can express this in the form $g_D(\bar{\mathcal{F}}_L^0 C \mathcal{F}_L^0 + L \to R)$ where C is the just the diagonal matrix

$$C = \begin{pmatrix} 0 & 0 & 0 \\ 0 & 1 & 0 \\ 0 & 0 & -1 \end{pmatrix} . \tag{13}$$

In the mass eigenstate basis this interaction then just becomes $g_D(\bar{\mathcal{F}}_L C_L \mathcal{F}_L + L \to R)$ where we define $C_{L,R} = U_{L,R} C U_{L,R}^\dagger$ with the elements of theses effective coupling matrices now given by $(C_R)_{ij} = U_{i2}^R U_{j2}^{R*} - U_{i3}^R U_{j3}^{R*}$ and similarly for $L \to R$ where $(i, j = 1, 2, 3)$ corresponds to the mass eigenstates f, F_1, F_2, respectively. Some obvious but important things to note about these matrices include: (i) off-diagonal couplings to the DP between the SM f and the VLF PM are generated allowing for decays such as $F_{1,2} \to fV$ with rates controlled by (the squares of) factors of order $m_i X_i/a_i$. (ii) f picks up a mixing-induced *diagonal* coupling to the DP proportional to g_D that is *not* vector-like, *i.e.*, parity-violating, since $U_L \neq U_R$. Explicitly we find, using the matrices above that $(C_R)_{11} = m_1^2 X_1^2/a_1^2 - (1 \to 2)$ while $(C_L)_{11} = m_f^2 X_1^2/a_1^2 - (1 \to 2)$ hence smaller by factors of $m_f^2/m_{1,2}^2$ which are $<< 1$ except possibly in the case when $f = t$ but even there this factor is still likely quite small. We will return to the implications of these couplings in our discussion below.

The mixing of f with the PM can also lead to alterations in the couplings of these fields to the SM W, Z bosons. In the Z boson case, since $f_R, F_{1,2R}$ are all iso-singlets, the rotation of these fields by the matrix U_R has no impact on their Z couplings; this is no longer true for the corresponding left-handed fields. In the original weak basis these fields couple as $\frac{g}{c_W}(T_{3f} C_Z - x_W Q_f I)$ where I is the 3×3 identity matrix, $x_W = \sin^2\theta_W$, T_{3f} is the usual third component of the weak isospin for the SM field f_L and C_Z is just

$$C_Z = \begin{pmatrix} 1 & 0 & 0 \\ 0 & 0 & 0 \\ 0 & 0 & 0 \end{pmatrix} . \tag{14}$$

The resulting elements of the LH-coupling matrix in the mass eigenstate basis then become $\frac{g}{c_W}(T_{3f} U_{i1}^L U_{j1}^{L*} - x_W Q_f \delta_{ij})$ with δ_{ij} the usual Kronecker delta. There are again several simple but important things to note: (i) for the SM f, the quantity proportional to T_{3f} now differs from unity by a term of order $m_f^2 X_i^2/a_i^2 << 1$ even for the top quark. Thus to a good approximation the couplings of the SM fields to the Z are left unaltered by the mixing with PM; a similar argument can be made for the W as well since the same factor of $U_{i1}^L U_{j1}^{L*}$ will also appear there. (ii) Off-diagonal couplings are generated such

that decays such as $F_{1,2} \to fZ$ (as well as $f'W$) are now allowed and are controlled by (the squares of) factors of order $m_f X_i/a_i$. Note that these factors (squared) are smaller by $\sim m_f^2/m_{1,2}^2 << 1$ than those controlling the decay $F_{1,2} \to fV$ described above; a similar suppression is observed in the case of the W. Hence the PM decays into the DP (and S as we will find below) will *far dominate* those into the conventionally sought W, Z final state modes. The impact of this will be discussed further in more detail below.

Finally, we note that something similar happens when we consider the fermion couplings to the SM Higgs, H[3]. In the weak basis this is just $\frac{\sqrt{2}m_f}{v_H}\bar{\mathcal{F}}_L^0 C_Z \mathcal{F}_R^0 H + h.c.$ using the notation above so that in the mass basis a coupling matrix, $C_H = U_L C_Z U_R^\dagger$, is produced whose elements are given by $(C_H)_{ij} = U_{i1}^L U_{j1}^{R*}$ and where we again see that the deviation of $(C_H)_{11}$ from unity is highly suppressed. Off-diagonal terms in C_H allow for the decays $F_{1,2} \to fH$ but these are found to have small (squared) couplings $\simeq m_f^2 X_i^2/a_1^2$ similar to those for the W, Z final states above so that these partial widths cannot remotely compete with those for $F_{1,2} \to fV$. This result should come as no surprise as this follows immediately from use of the Goldstone Boson Equivalence Theorem [15]. In a similar manner, we can determine the corresponding coupling of the remaining real dark Higgs scalar, S, to the various fermions that are induced by the off-diagonal coupling above; we can express this result simply as $\beta_{ij} = [U_{i2}^L \lambda_1/\sqrt{2} + U_{i3}^L \lambda_2/\sqrt{2}] U_{j1}^{R*}$.

3.1 Leptonic Portal Matter

We now turn to an examination of some sample implications of the above mixing and generated couplings for several choice of f. We first consider the case of a VLL, *i.e.*, $F = E$, so that $f = e$ above; in this case $U_L \simeq I$ (at least as far as the ee and $eE_{1,2}$ elements are concerned) due to the small value of m_e relative to all the relevant mass scales and so we can completely neglect LH-mixing as far as SM fields are concerned in the rest of the present discussion. However, the RH-mixing is still active so that, collecting the various pieces, *e.g.*, the coupling of the electron to the DP is now given by

$$\big[- e\epsilon\ \bar{e}\gamma_\mu e + g_D (C_R)_{11}\ \bar{e}\gamma_\mu P_R e \big] V^\mu \equiv -e\epsilon\ \bar{e}\gamma_\mu (v_e - a_e \gamma_5) e V^\mu \,, \tag{15}$$

where $v_e = 1 - y$ and $a_e = -y$ with $y = g_D (C_R)_{11}/2e\epsilon$. One might roughly expect that $(C_R)_{11} \simeq X_i^2/m_i^2 \simeq 10^{-4}$ in the present case based on the arguments above so that, very roughly, $0.01 \lesssim |y| \lesssim 0.5$ and thus the DP may mediate a reasonably strong parity-violating interaction for the electron. This possibility may be probed by a number of low-energy (*i.e.*, low momentum transfer, $Q^2 \lesssim m_V^2$) experiments such as in atomic parity violation (APV) [16] or in polarized electron-electron/electron-proton scattering [17]. In the case of APV, the amount of parity violation is quantified by a parameter Q_W, the weak charge, which in the SM is just $-(A - Z) + (1 - 4x_W)Z \simeq -73.23(1)$ [18] for the case of Cesium ($Z = 55, A = 133$) whereas the experimental value is -72.62(43) [18]. DP exchange in the present setup produces an additional contribution to Q_W given by:

$$\Delta Q_W^V = \frac{-8\sqrt{2}\pi\alpha\epsilon^2}{G_F m_V^2} y Z \frac{m_V^2}{Q^2 + m_V^2} \,, \tag{16}$$

where G_F is the Fermi constant and which is given numerically (with $Q^2 \to 0$) by

$$\Delta Q_W^V(Cs) \simeq -1.22\ y \left(\frac{100\text{MeV}}{m_V}\right)^2 \left(\frac{\epsilon}{10^{-4}}\right)^2 , \tag{17}$$

which must satisfy the constraint $-0.23 \leq \Delta Q_W^V \leq 1.45$ at 95% CL to be consistent with the current experimental result. This is quite easily done for values of $|y|$ in the above range of interest even for correspondingly respectable ranges in the values of both the parameters m_V and ϵ. Polarized Moeller scattering [17], on the otherhand, will be much more sensitive probe of $y \neq 0$ as it leads to an apparent shift in the effective value of the weak mixing angle which can be written as

$$\Delta x_W \simeq 5.56 \cdot 10^{-3}\ y \left(\frac{100\text{MeV}}{m_V}\right)^2 \left(\frac{\epsilon}{10^{-4}}\right)^2 \frac{m_V^2}{< Q^2 > + m_V^2} \,, \tag{18}$$

[3]We have set the $H - S$ mixing exactly to zero for this discussion due to the constraints mentioned above.

with $< Q^2 >$ being effective average value of Q^2 probed by the experiment which in this case is $\simeq$ (75 MeV)^2 [16,17]. Assuming that the SM value is realized at the end of this experiment, this will result in a constraint $|\Delta x_W| \leq 5.6 \cdot 10^{-4}$. For $m_V = 100(300)$ MeV with $\epsilon = 10^{-4}$ this will imply a bound of $|y| \leq 0.16(1.2)$ which we again see can be easily satisfied. Quite generally, however, this experiment is observed to be able to probe a reasonable portion of the parameter space of this particular setup; of course a result in conflict with SM expectations would prove most interesting.

In the case where PM is muon-like instead of electron-like, *i.e.*, $F = M$, one might ask if the added flexibility allowed by $y \neq 0$ could help explain the anomaly in the muon's value of g-2; this question is easily addressed employing the general results given in [19]. There are actually several new contributions at the 1-loop level to this quantity beyond the one usually appearing in DP models. Ordinarily in such models the lone contributing diagram has a DP loop with the SM photon emitted off the internal muon line and where the DP coupling to the muon is both diagonal and purely vectorial; such a graph is usually simply suppressed by the small value of ϵ^2. In the present scenario such a diagram exists but both vector and axial-vector couplings are now present. Generally the axial-vector contribution is found to add destructively with the one arising from the vector coupling making it less likely to explain the observation. Furthermore, this axial-vector contribution tends to be the larger one so that the sum of both contributions is negative yielding the wrong sign from what is needed to explain the deviation from the SM. Employing the notation above we find the sum of these two contributions can be expressed as

$$\Delta g_\mu^{V_1} = 2.32 \cdot 10^{-11} \Big(\frac{\epsilon}{10^{-4}}\Big)^2 \int_0^1 dx \; \frac{x(1-x)[x(1-y)^2 - (4-x)y^2]}{x^2 + r(1-x)} \tag{19}$$

where $r = m_V^2/m_\mu^2 \sim 1$ and explicitly shows the opposite sign contribution arising from the axial-vector coupling term. The integral is usually < 1 so that this overall contribution is quite small for our default parameter choices; for example, taking $r = 1$ one obtains the rather small values $\simeq 0.105(1-y)^2 - 0.732y^2$ for the integral and which can be of either sign depending upon the value of y. To obtain a more general understanding of this result, we can rewrite the expression above as

$$\Delta g_\mu^{V_1} = 10^{-11} \Big(\frac{\epsilon}{10^{-4}}\Big)^2 R(y, m_V)\,, \tag{20}$$

where the quantity R is shown in Fig. 1 as a function of m_V for various values of y. Clearly, R is almost always negative and only yields at most a small overall contribution to the g-2 of the muon.

In addition to these 'standard' DP contributions, there are now also a pair of 1-loop graphs with either a DP or a dark Higgs loop where the internal line is a PM state, M_i, and the couplings at both vertices are chiral. For these contributions the strong suppression is now the result of the rather small value of the ratio m_μ^2/m_i^2 for the typical values of the PM masses that we might expect. In the scalar case we find (since $m_S^2 << m_i^2$) that a positive result is obtained, *i.e.*,

$$\Delta g_\mu^S = 5.85 \cdot 10^{-10} \sum_i \frac{X_i^2}{v_s^2} \Big(\frac{200\text{GeV}}{m_i}\Big)^2\,, \tag{21}$$

which, since $|X_i|/v_s \sim 1/2$, is roughly an order of magnitude too small to make an important contribution unless the values of m_i are significantly smaller than we might expect. For the corresponding DP graph with a PM on the internal line, we instead obtain

$$\Delta g_\mu^{V_2} = -2.35 \cdot 10^{-4} \left(\frac{g_D}{0.1}\right)^2 \left(\frac{100\text{MeV}}{m_V}\right)^2 \sum_i \Big(\frac{X_i^2}{m_i^2}\Big)\,, \tag{22}$$

where we have used the fact that $m_i^2 >> m_{V,\mu}^2$ and that $|(C_R)_{1i}| \simeq |X_i|/m_i$ to leading order in the small mass ratios. Given the estimates above this contribution will also yield a *negative* result but only as most as large as O(10^{-11}), similar to the first DP contribution above.

It is interesting to now very briefly consider how this singlet electron- or muon-like PM case differs from an alternative setup where the PM fields form the VLL $SU(2)_W$ doublet $(N, E)^T$ (or $(N, M)^T$).

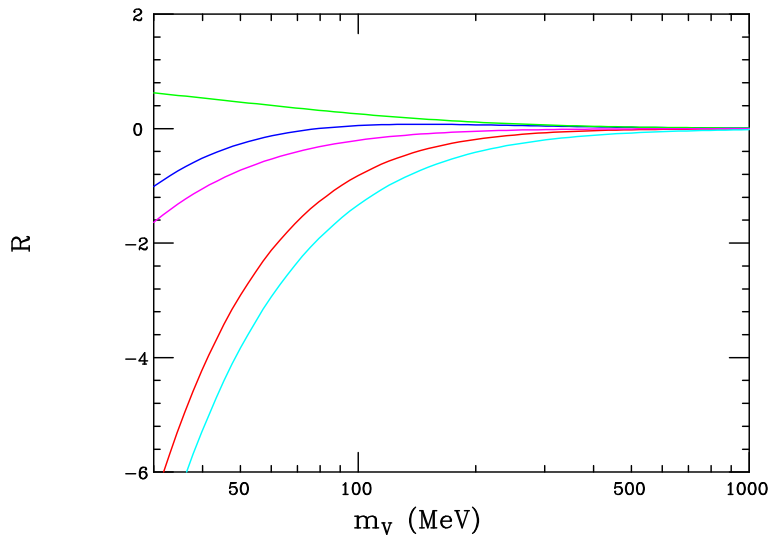

Figure 1: The parameter R, as defined in the text, as a function of the DP mass m_V assuming $y = -0.5(-0.25, 0, 0.25.0.5)$ corresponding to the red(blue, green, magenta, cyan) curves, respectively.

In the $Q = -1$ sector, all of the analysis presented in the previous discussion, with the interchange of LH- and RH-labels, essentially remains unaltered except that $y \to -y$. The presence of the $Q = 0$, N, however, brings us something new. First, note that due to $SU(2)_W$ the weak states N_i and E_i will have essentially the same masses so that the U_L matrices for both the $Q = 0, -1$ sectors will be the same. This implies, in the limit that lepton masses can be neglected, that there is no new physics in the charged current sector coupling to $W^{\pm}$. However, the mixing of N with the ordinary LH SM ν field now induces a coupling of this SM ν field to the DP of the form

$$2e\epsilon y \; (\bar{\nu}\gamma_\mu P_L \nu) \; V^\mu \,, \tag{23}$$

which may lead to observable effects in low energy neutrino experiments provided that the typical $< Q^2 >$ is not very much larger than m_V^2 [20]. We note in passing that when finite m_V^2/m_Z^2 corrections are included in the usual DP model (where PM effects are not considered), couplings to the neutrino are also induced as well but then these have a strength suppressed by this very small mass ratio in comparison to $e\epsilon Q$. These couplings are far smaller than the ones that can potentially be induced by mixing of the SM fields with the PM since $|y|$ can be sizable as discussed above. This possibility will be explored elsewhere [21].

3.2 Hadronic Portal Matter

Now let us turn our attention to the case where the PM fields carry color. Here we mainly focus on the specific example of the bottom-like singlet VLQ, *i.e.*, $F_i = B_i$. While the case $F_i = T_i$ shares some features with this possibility, it has many unique aspects of its own which we will briefly discuss and contrast with the $F_i = B_i$ scenario below. For $F_i = B_i$, the general analysis presented above remains applicable as $m_b^2 << m_{1,2}^2$. Instead of flavor physics and low-energy phenomena, here we will be more interested in B_i production and decay at the LHC especially as we anticipate that roughly $m_{1,2} \sim 1 - 2$ TeV in this case[4].

We first examine the usual QCD pair-production mechanism which is model-independent except

[4]Of course, if there were additional flavor symmetries active, the implications on low energy phenomenology of such states could also be very interesting.

for the values of $m_{1,2}$. To set the scale for the overall event rate, note that at $\sqrt{s} = 13$ TeV the production cross section for $\bar{B}B$ production at the LHC would be roughly $\simeq 42(2.0, 0.60, 0.25)$ fb for $m_B = 1(1.5, 1.8, 2)$ TeV [22], respectively, as shown in the top panel of Fig. 2. Generally, for this interesting mass range, this cross section is seen to scale roughly as $\sim m_B^{-7}$ so that values for other nearby masses can be easily obtained. This also implies that if $m_{B_2}/m_{B_1} = 1.5(1.8)$ then $\sigma(B_2)/\sigma(B_1) \lesssim 0.06(0.02)$ so that almost the entire signal would arise from the lighter of the two states. As noted above (and as now applied specifically to this example), one easily finds that the partial decay widths for conventional modes such as $B_i \to bZ, bH$ and $B \to tW$ to be quite highly suppressed in comparison to the partial widths for decays to the bV, bS final states, vanishing completely in lowest order in the $m_b \to 0$ limit. This implies that the ordinary modes usually employed at the LHC in the searches for VLQ are *inoperable* in this case. How do the partial widths for the $B_i \to bV, bS$ decay modes compare? We first recall that the B_i are likely to have somewhat comparable masses such that $m_{1,2}^2 >> m_b^2, m_{S,V}^2$ since both $m_{V,S}$ are $\sim$ a few GeV at most. In the limit where we can neglect all of the light particle masses appearing in the final state we find that the partial widths for both the V, S modes are identical (again this is due to the Equivalence Theorem [15]) and are given in the small mixing angle limit by

$$\Gamma(B_i \to bV, bS) = \frac{\lambda_i^2 m_i}{32\pi}\,, \tag{24}$$

where the λ_i have been defined above and are nominally of O(1). These decays are clearly prompt even for substantially smaller values of the λ_i's. It is important to remind ourselves of the lifetimes of the S, V states that appear here as B_i decay products. The well-known total decay width for V can be written in terms of its partial width into e^+e^- and the branching fraction for this mode, $B_e(m_V)$, as (taking here the $m_e^2/m_V^2 \to 0$ limit for simplicity given the V mass range of interest below)

$$\Gamma(V \to all) = \frac{\alpha\epsilon^2 m_V}{3B_e} = 2.432 \cdot 10^{-9} \left(\frac{\epsilon}{10^{-4}}\right)^2 \left(\frac{m_V}{100\text{MeV}}\right) \frac{1}{B_e} \text{ MeV}\,, \tag{25}$$

which corresponds to an *un-boosted* decay length for V of

$$c\tau \simeq 81.44 \left(\frac{10^{-4}}{\epsilon}\right)^2 \left(\frac{100 \text{ MeV}}{m_V}\right) B_e \ \mu m\,. \tag{26}$$

Now recall that $m_V/m_S = g_D/\sqrt{2\lambda_S}$ so it is very likely that $m_S > m_V$ and we will assume that this is true in what follows. When $m_S > 2m_V$, then the dominant S decay is naturally $S \to VV$ with a partial width given by[5]

$$\Gamma(S \to VV) = \frac{g_D^2 m_S}{128\pi} \frac{1}{x_V} (1 - 4x_V)^{1/2} (1 - 4x_V + 12x_V^2)\,, \tag{27}$$

where $x_V = m_V^2/m_S^2$ and this is also seen to be a prompt decay, even near threshold. If instead we have that $m_V < m_S < 2m_V$, we obtain a partial width of

$$\Gamma(S \to Ve^+e^-) = \frac{g_D^2 \alpha\epsilon^2 m_S}{96\pi^2}\ F(r) = 7.7 \cdot 10^{-16}\ m_S \left(\frac{g_D}{0.1}\right)^2 \left(\frac{\epsilon}{10^{-4}}\right)^2 F\,, \tag{28}$$

where here $1/2 < r = m_V/m_S = \sqrt{x}_V < 1$ and F is a well-known function [23] that ranges over many orders of magnitude and whose behavior we display in the lower panel of Fig. 2. We note, for example, that for $r = 0.6(0.7, 0.8, 0.9)$ one finds that $F = 0.443(5.55 \cdot 10^{-2}, 4.97 \cdot 10^{-3}, 1.18 \cdot 10^{-4})$, respectively, so that F falls off rapidly with increasing r, that can lead to a very substantial width suppression/lifetime lengthening due to phase-space. Of course, very close to the VV threshold finite V width effects will become important here but as noted above the V total width itself is quite small due to the appearance of the overall ϵ^2 suppression. Thus it is clear that this $S \to Ve^+e^-$ partial width is extremely small so we must take some care that S has no other possible decay modes than may compete, *e.g.*, through the very suppressed mixing with the SM Higgs via a tiny, but non-zero value of λ_{HS} as discussed above. For

[5] Recall that in the present setup, S has no tree-level allowed decay to DM assuming that such a mode is even kinematically open.

example, the $H - S$ mixing-induced partial width for $S \to l^+l^-$ is just

$$\Gamma(S \to l^+l^-) \simeq \frac{G_F m_l^2 m_S}{4\sqrt{2}\pi}\ \beta_l^3 \theta_{HS}^2 \lesssim 2.4 \cdot 10^{-16} m_S\,, \tag{29}$$

where in the last step we consider the case of $l = \mu$, have set the phase space factor $\beta_l \to 1$ and employed the upper limit on the value of θ_{HS} discussed above with $v_s/v_H = 10^{-2}$ and assumed an invisible Higgs branching fraction of $B_{inv} = 0.1$. (The corresponding partial width into e^+e^- is smaller by roughly a factor of $4.3 \cdot 10^4$.) Here we see that if S lies above the $\mu^+\mu^-$ threshold and we saturate the LHC bound on the $H - S$ mixing coming from SM Higgs decay then the rate for the $S \to \mu^+\mu^-$ decay may be comparable to or even dominate over that for Ve^+e^- especially since F is potentially very small. Here we will *assume* that this is *not* the case but we proceed with this caveat in mind. Inserting typical values

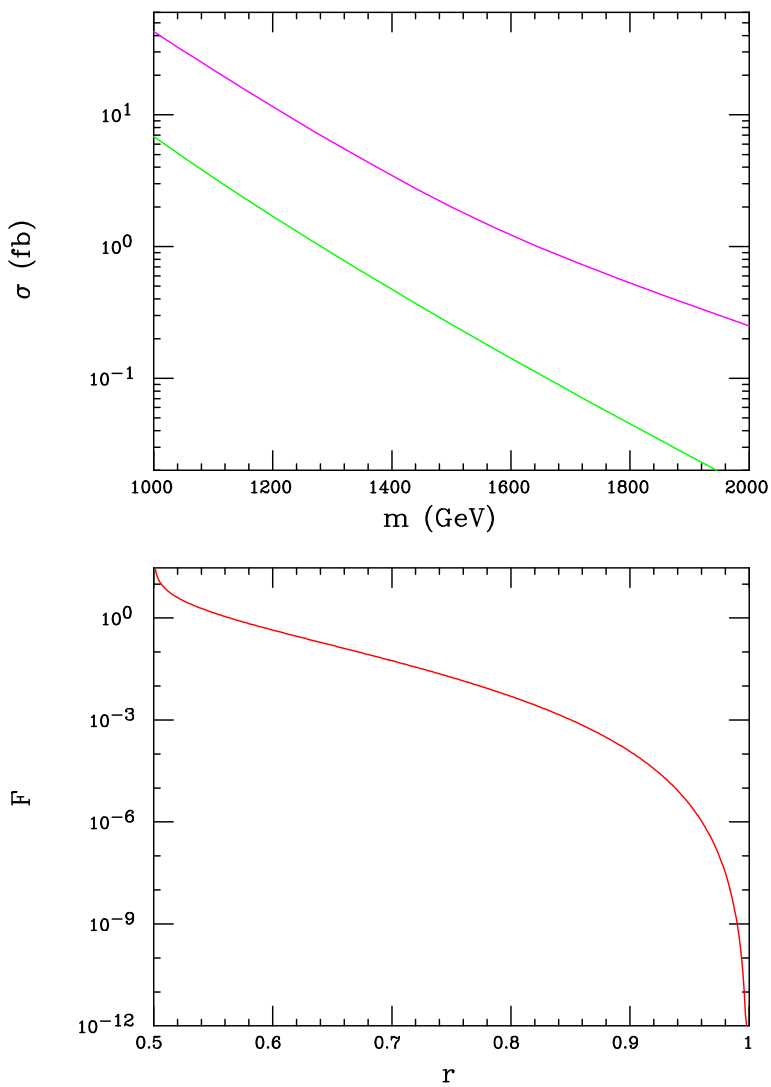

Figure 2: (Top) $B\bar{B}$ (magenta) and b-squark (green) pair production cross section at $\sqrt{s} = 13$ TeV as discussed in the text. (Bottom) Values of the 3-body phase space function F for the decay $S \to Ve^+e^-$ as a function of $r = m_V/m_S$ as described in the text.

into the above expression for the $S \to V e^+ e^-$ partial width leads to an *un-boosted* S decay length for masses in the relevant interval of

$$c\tau \simeq 170.8 \left(\frac{0.1}{g_D}\right)^2 \left(\frac{10^{-4}}{\epsilon}\right)^2 \left(\frac{150 \text{ MeV}}{m_S}\right) \frac{1}{F(r)} \text{ cm}\,. \tag{30}$$

From these estimates it would seem that bottom-like PM (generically B for simplicity) pair-production at the LHC would produce quite unusual events in certain phase space regions, *i.e.*, the apparent signatures for B pair production depend critically upon where one sits in the model parameter space. Perhaps the simplest situation is where both the B and $\bar{B}$ each promptly decay into a DP, *i.e.*, the $b\bar{b}VV$ final state. Since the B's are presumed heavy and relatively slow their decay will yield two, high p_T, b-jets (that can act as the trigger) that are generally *not* back to back. Both V's will be very highly boosted and also likely not back to back, each sharing the parent B rest energy with the associated b-jet, so that $\gamma_V \simeq m_B/2m_V \sim 5000(1000)$ if $m_V = 100(500)$ MeV and $m_B = 1$ TeV; the boost is, of course, larger if B is more massive. To get a rough idea of the resulting decay properties and *boosted* decay lengths ($d = \gamma_V \beta c\tau$) of the DP within the interesting parameter space region we perform the following scan: (i) we take ϵ to lie in the range $10^{-5} - 10^{-3.5}$ while, independently, (ii) m_V lies in the range $10^{1.5} - 10^3$ MeV. Specific values in these ranges are chosen employing log priors. Once m_V is known we can then estimate the value of B_e [24] and hence determine the quantity of interest, d, using the equation above. We note that the low-mass end of this range where ϵ is simultaneously chosen to also be at the lower end of its range is somewhat disfavored by existing experiments [5]. We do *not* account for this as part of this scan but point out that it is in this region that the longest V lifetimes (and corresponding boosts) are frequently obtained. Given these numerical assumptions and caveats, the result of this scan for 10^7 generated model points is shown as the histogram in the top panel of Fig. 3. For these assumed parameter ranges, the peak of this distribution is seen to lie roughly at $d \sim 0.7$ m but the distribution of possible values for d is observed to have quite long, slightly asymmetric tails going down to values of $d \sim 2$ mm and up to $d \sim 400$ m. In all cases $m_B = 1$ TeV has been assumed; larger mass values will lead to correspondingly increased boosts but only by a small factor. Of course, any given model point in this parameter space will realize only a *specific* d value within this range. We note the trivial observation that for a fixed value of d, the two V's in the final state can generally decay at different distances from the IP and these may even occur in different LHC detector elements.

For those regions of the parameter space where *both* V decays will most likely occur long after they leave the detector, such events would likely appear (incorrectly) as having missing E_T (MET) in addition to the two b-jets. This is a 'conventional' signature that is essentially covered by the usual SUSY direct b-squark decay to bottom plus the LSP searches [25], albeit with somewhat different production cross sections and acceptances[6]. The present null results for these searches certainly would imply that $m_{1,2} > 1 - 1.5$ TeV in such cases. If we had instead considered the top-like PM, T, which would similarly decay to a tV final state with a very long lived V, such signatures would be then be covered by the analogous top squark searches leading to somewhat similar mass constraints on the PM. Of course, if a secondary, 'far' detector were to be available at an appropriate distance, such as MATHUSALA [28], a larger fraction of these long-lived particle decays might be captured and studied. Perhaps more interesting are events where one or both of the V's decay before/inside the calorimeter/muon system after leaving no tracks in the inner detector. If even one of the V's decay after leaving the detector, the event will still appear as two b-jets plus MET but with additional activity due to the other V now decaying inside the detector.

Obviously, if both V's decay inside the detector there will be no MET signature but the high p_T b-jets can still provide the necessary trigger. If both/either V decays into SM particles (*e.g.*, e^+e^-, $\mu^+\mu^-$, $\pi^+\pi^-$) *inside* the detector it will appear as a long-lived/displaced lepton-jet [29] and this has frequently been discussed as a dark sector signature (as it is here) although generally in kinematic regimes with significantly smaller boost values. Searches for such lepton-jet final states within the context of specific signals models have been performed by both ATLAS and CMS at the LHC [31] with null results[7]. For

[6]Note that the total b-squark pair production cross section in this mass range for decoupled gluinos is roughly a factor of $\sim 6 - 10$ smaller than is that for $B\bar{B}$ pairs [26, 27] as shown in the upper panel of Fig. 2.

[7]Note that the corresponding appearance of *prompt* lepton-jets are not very likely for the V, S final states in the current setup due to the rather large boosts that are generally expected here. However, such searches *may* still play important roles

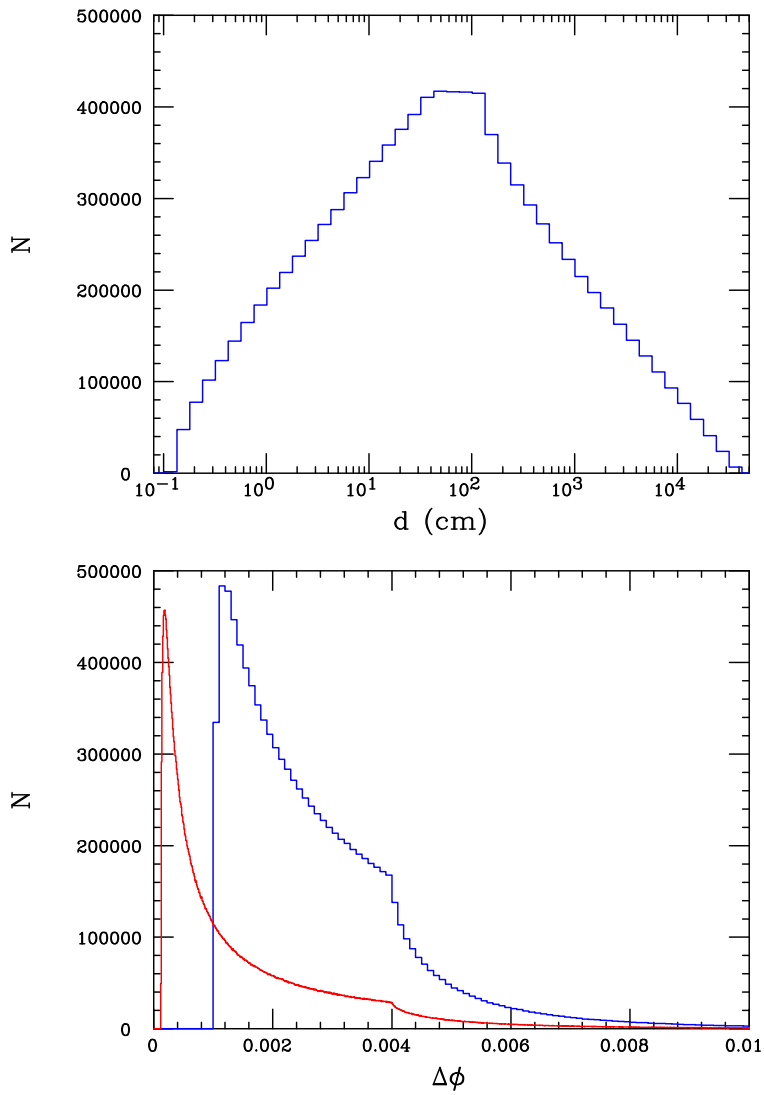

Figure 3: (Top) Boosted decay length (d) distribution of the DP from the decay $B \to bV$ assuming that $m_B = 1$ TeV as described in the text. (Bottom) Boosted leptonic opening angle distributions, averaged over the model parameter space, for the boosted $V \to e^+e^-$ (red) and $V \to \mu^+\mu^-$ (blue) decay modes.

this decay mode, the opening angle between the V decay products will be very small due to the large boost that the V experiences from the parent B decay. These are shown in the lower panel of Fig. 3 for the both e^+e^- and $\mu^+\mu^-$ final states which represented the parameter space weighted averages for these expectations (and not those associated with a specific parameter choice). For the $\mu^+\mu^-$ final state case we added the additional constrain that $m_V \geq 250$ MeV as part of the scan while $m_e = 0$ has been assumed throughout. Since displaced lepton-jets decaying at different depths in the detector are somewhat difficult to simulate with DELPHES [29,30], we can obtain an (extremely crude) estimate for the *largest* possible rate for such events by assuming that, *e.g.*, ATLAS is a perfect detector of radius 7m with 100% acceptance and efficiency so that any $V \to$ lepton-jet events produced inside this detector volume are observed. Assuming an integrated luminosity of 100 fb^{-1} for purposes of demonstration, knowing the $B\bar{B}$ cross section and the distribution of values of d from above, we can ask what is the maximum number of single lepton-jet events that might be observed under these extremely optimistic assumptions (assuming both the bV and bS final states produce at least one lepton-jet) as a function of d. The result of this calculation, which is clearly a sizable overestimate of reality, is shown in the upper panel of Fig. 4. From this result we can argue that for values of d below ~ 10's of meters lepton-jets from B-like MP in the mass range of interest may likely be observable with the Run II data set. Of course a much more realistic analysis of this possibility is clearly extremely necessary.

When the decay $B \to bS$ occurs the critical issue is whether or not the bound $1 < m_S/m_V < 2$ is satisfied; although this appears to be a small region of the parameter space, it is the one most analogous to that realized in the SM for the Higgs and $W^\pm$ so we need to take this possibility quite seriously. If the mass ratio does lie in this range, when S receives a boost of $\sim 10^3 - 10^4$ from the original B, the boosted decay length of S can easily exceed $\sim 10 - 100$ km as its un-boosted decay length is typically $\sim 2/F$ m as discussed above. This result is shown in the lower panel of Fig. 4 which makes use of the previous parameter space scan and, in addition, now includes an additional scan over values of $1 < m_S/m_V < 2$ with a flat prior. Here the function $F(r)$ plays a rather significant role in increasing both the S lifetime and the corresponding boosted decay length. In such a situation it is quite likely that the V's from S decay will themselves decay to SM particles very far outside the detector. In such cases we return to the two b-jet plus MET signature as previously discussed and which yields a bound of $m_{1,2} > 1 - 1.5$ TeV or more. We note that if $H - S$ mixing *is* important at the level discussed above, and if $S \to \mu^+\mu^-$ is kinematically open, then its un-boosted decay length will be greater than ~ 0.55 m; such values would still lead to quite long boosted decay lengths and result in the likely decay of S outside of the detector much of the time.

When $m_S > 2m_V$, on the other hand, the $S \to VV$ decay is prompt resulting in a two b-jet plus $4V$ final state with the two pairs of V's from each S being strongly columnated due to the large boost. Since the V's in such a case result from a secondary decay in the chain and their pre-boost velocities can be oriented arbitrarily (with a flat distribution with respect to the motion of the S since it is spin-0), their actual boosts will be somewhat reduced. In this case the secondary V boosted decay lengths, shown in the top panel of Fig. 5, will be somewhat shorter than when the V arises directly from $B \to bV$. (To obtain these numerical results we have assumed that $2 \leq m_V/m_S \leq 5$ with a flat prior.) Note that some of the V decays in this parameter space region may now appear as *prompt* unlike when $B \to V$ directly. This d distribution is now seen to display a peak value of ~ 30 cm but, again, with rather long tails, extending below ~ 1 mm at the lower end. The two V's from a given S may not decay at the same time or possibly even in the same region within the detector since the ratio of the *distinct* boosts that the V's receive from the $B \to S \to VV$ decay chain can be O(1), this again due to the random orientation of the produced V relative to direction of the moving S. The lower panel of Fig. 5 shows the ratio of these two boosts where V_1 is always defined as the one obtaining the larger boost in this decay chain. We see that while a ratio of unity is the most likely value, there is a large region of this model space where this ratio is significantly greater than unity. On average, employing the same scan results as above, we find that the opening angle between the two V's in the detector is generally still quite small as seen in Fig. 6. It is to be remembered that this result represents the weighted distribution for this opening angle averaged over the model parameter space and is *not* that corresponding to a specifically chosen parameter space point.

in certain corners of the parameter space.

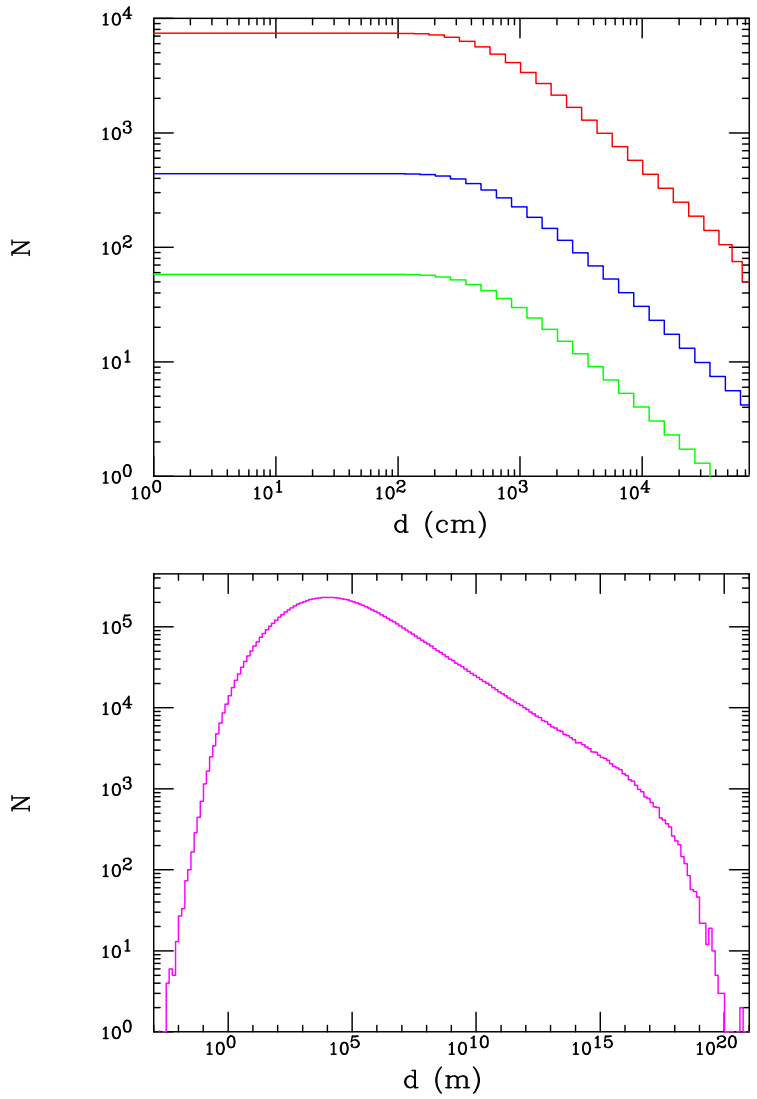

Figure 4: (Top) Event rate estimate for the number of single lepton-jets for the idealized ATLAS detector as discussed in the text assuming an integrated luminosity of 100 fb^{-1}. From top to bottom the histograms assume that $m_1 = 1, 1.5, 2$ TeV, respectively. (Bottom) Boosted decay length (d) distribution of the S from the decay $B \to bS$ assuming that $m_B = 1$ TeV as described in the text assuming $m_V < m_S < 2m_V$.

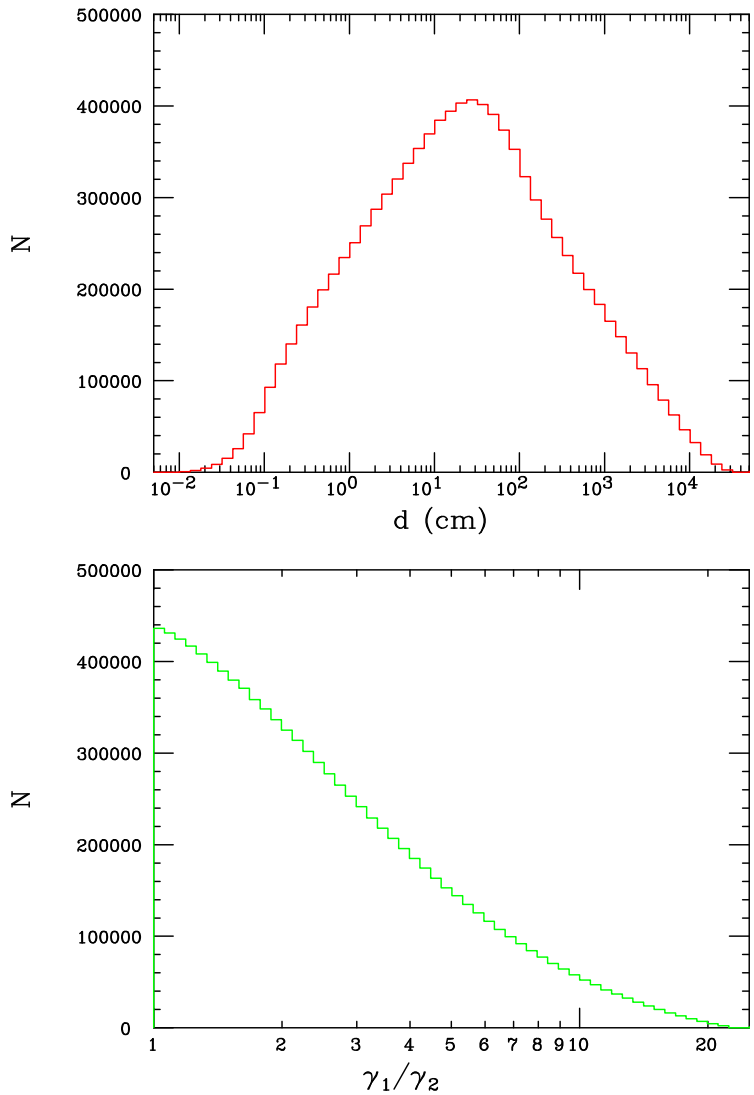

Figure 5: (Top) Boosted decay length (d) distribution of the V arising from the decay chain $B \to bS, S \to VV$ assuming that $m_B = 1$ TeV as described in the text. (Bottom) Ratio of the boosts of the two V's produced from a single initial B (or $\bar{B}$) and the $B \to bS, S \to VV$ decay chain. V_1 is always defined to be the state with the larger boost.

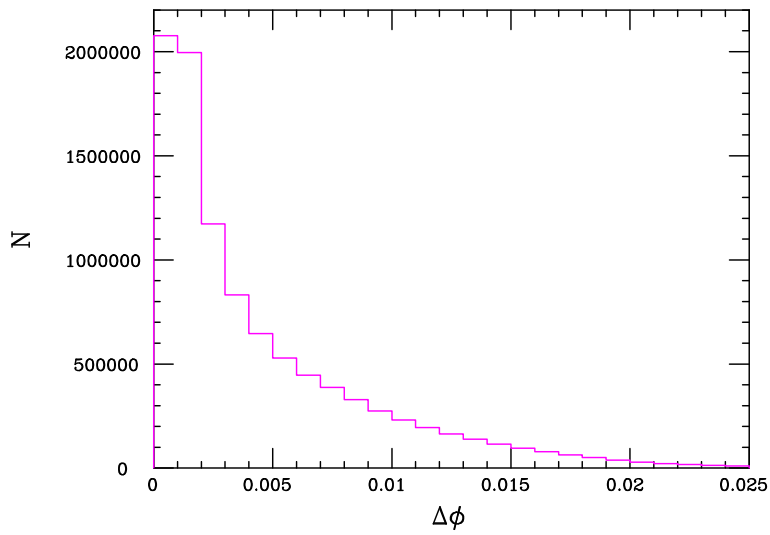

Figure 6: Distribution of the opening angle between the two V's in S decay, $\Delta\phi$, as described in the text.

In addition to $B\bar{B}$ pair production, we briefly note that single B associated production with V/S can also occur at a significant rate for λ_i being O(1) with a LO cross section that is given by (in the limit $m^2_{b,V,S} \to 0$)

$$\frac{d\sigma}{d\hat{t}} = \frac{\lambda_i^2 \alpha_s}{48\hat{s}^2}\Big[\frac{(\hat{s}+\hat{t})^2}{-\hat{s}t'} + m_i^2(\hat{s}+\hat{t})(\frac{1}{\hat{s}^2}+\frac{1}{t'^2}) - \frac{2m_i^2\hat{t}}{t'}(\frac{2}{t'}+\frac{1}{s})\Big]\,, \tag{31}$$

where $t' = \hat{t} - m_i^2$; note that in this limit, the Equivalence Theorem [15] tells us that production with either S or V yields the same cross section. We note that in the corresponding case where $F_i = T_i$ such a production mechanism is absent. The value of this associated production cross section at the $\sqrt{s} = 13$ TeV LHC is shown in the top panel of Fig. 7 as a function of the B_i mass for different p_T cuts on S, V and as a function of $p_T^{min}(S,V)$ for different choices of the B_i mass; in all cases a cut $|\eta_{V,S}| < 2.5$ has been applied. This associated production process, as in the case of $B\bar{B}$ production, leads to a very highly boosted V, S arising from the B decay itself. However, the *associated* V, S, which is also produced in this process, generally arrives with lower p_T and at larger rapidities, as can be seen in the lower panel of Fig. 7 and in Fig. 8. Thus for fixed p_T this V, S is likely to experience a somewhat smaller boost especially at the smaller rapidities, $|\eta_{V,S}| \to 0$, in comparison to those produced in the B decay. In particular we see that, for the range of masses of interest to us, almost all the events are found to lie in the region $|\eta_{V,S}| \gtrsim 0.5 - 1$.

Finally we note that the possibility of the $\bar{B}B \to \bar{b}b + SS/VV/VS$ final state at the LHC is just one example of what may happen for any of the $\bar{F}F$ PM final states discussed above. As mentioned earlier one should also insure that the $\bar{t}t + S, V$ final state is also explored since it is qualitatively similar to the case of $F = B$ except that top reconstruction is somewhat less efficient than is the tagging of high p_T b-jets. Also, one should not ignore the pair production of the *leptonic* MP states at the LHC through their electroweak interactions which can have sizable rates at somewhat lower masses and that can lead to MET $+V, S$ when $F = N$ or opposite sign, same flavor leptons $+V, S$ final states when $F = E, M$.

4 Summary and Conclusions

The generation of the kinetic mixing between the dark photon and the hypercharge gauge boson of the Standard Model is a necessary element in the construction of the dark photon mediator model. To

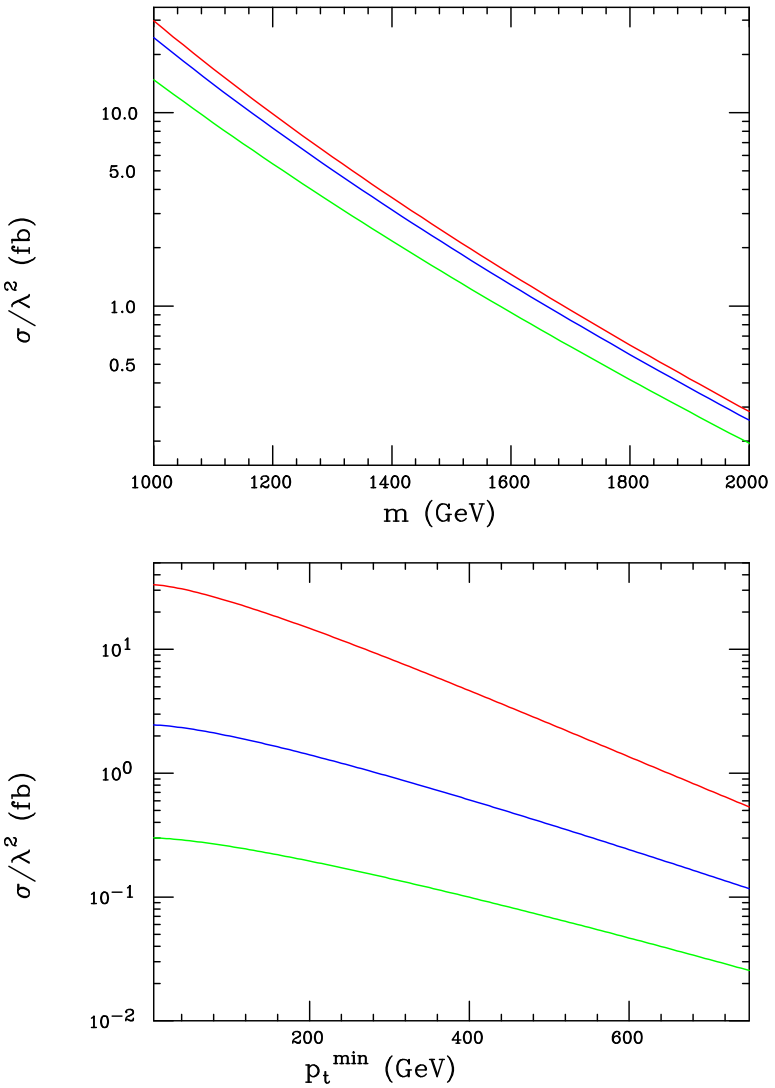

Figure 7: (Top) LO cross section for single B production in association with S/V as a function of the B mass. From top to bottom a cut of $p_T(S,V) > 50, 100, 200$ GeV, respectively, has been applied. (Bottom) Same as in the top panel but now as a function of $p_T^{min}(S,V)$ for, from top to bottom, a B mass of 1, 1.5, or 2 TeV, respectively, has been assumed. In both panels a cut of $|\eta_{V,S}| < 2.5$ has also been applied.

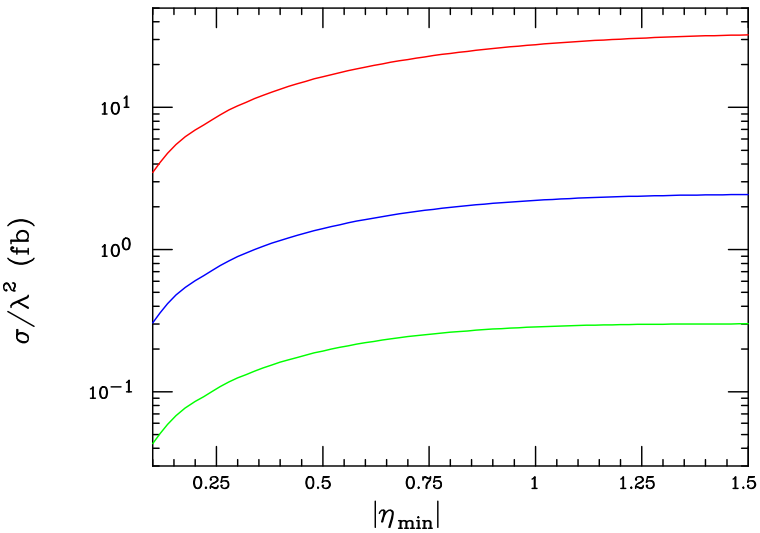

Figure 8: Associated production cross section for $B + V/S$ as a function of the $|\eta_{V,S}|_{min}$; from top to bottom, we assume a B mass of 1, 1.5, or 2 TeV, respectively.

accomplish this KM requires the existence of portal matter simultaneously carrying both dark and SM charges and if this matter is fermionic, as we argue above, it must be vector-like to avoid anomalies and the experimental constraints from arising from both precision electroweak data and Higgs decays. Among the set of possible SM transformation properties for these states, one can only chose from among those that allow for the PM to decay. This being the case, we demonstrated that the only way to do this at tree-level, given that the dark Higgs is a SM singlet, is to require that the PM transform as vector-like versions of the SM fields themselves. Of these five possible states, those that are also singlets under the $SU(2)_W$ gauge group presents us with the simplest possibilities and it is these cases that we have mainly focussed on here. However, it is quite likely that in more UV-complete frameworks the PM may be some more complex and interesting combination of these different vector-like states. In particular, we have found that if the PM and the dark Higgs, which is responsible for generating the mass of the DP, carry the same dark charge, then the vev of the dark Higgs will induce a mixing between the PM and the analogous SM field carrying the same SM quantum numbers thus allowing for the desired decay path. This same mixing leads to parity violating DP couplings to the SM fields which are the conventional analogs of the PM. If the PM transforms like the e_R, these parity-violating interactions may be probed by, *e.g.*, the MOLLER experiment. Similarly, if the PM transforms as μ_R, this same mixing will also lead to potential new contributions to the muon's g-2. This mixing is, in particular, also responsible for the specific prompt PM decays $F \to fV, S$, which are the (by far) dominant modes for these new states, that can be observable at colliders. As we have shown, although these MP are VLF, they do not decay into the familiar and usually sought $H, W^\pm$ or Z final states with any significant branching fractions so that these final states are *not* the ones to be employed in searching for PM. Here we discussed in the analysis above the specific case when the PM transforms as b_R, which leads, in the case of PM pair production, to b-jet pairs plus possible MET or, more interestingly, b-jets plus very highly boosted displaced lepton-jet signals at the LHC.

The exploration of the physics of PM as discussed above is just at its beginning stages and there are several directions which can be pursued.

Acknowledgements

The author would like to particularly thank J.L. Hewett as well as the members of the SLAC ATLAS Collaboration, in particular, Su Dong, C. Young, M. Diamond, R. Bartoldus, M. Kagan, C. Vernieri and A. Schwartzman for very valuable discussions on long-lived particles and lepton-jets in ATLAS. This work was supported by the Department of Energy, Contract DE-AC02-76SF00515.

References

[1] M. Kawasaki and K. Nakayama, Ann. Rev. Nucl. Part. Sci. **63**, 69 (2013) [arXiv:1301.1123 [hep-ph]].

[2] P. W. Graham, I. G. Irastorza, S. K. Lamoreaux, A. Lindner and K. A. van Bibber, Ann. Rev. Nucl. Part. Sci. **65**, 485 (2015) [arXiv:1602.00039 [hep-ex]].

[3] For a recent review of WIMPs, see G. Arcadi, M. Dutra, P. Ghosh, M. Lindner, Y. Mambrini, M. Pierre, S. Profumo and F. S. Queiroz, arXiv:1703.07364 [hep-ph].

[4] J. Alexander *et al.*, arXiv:1608.08632 [hep-ph].

[5] M. Battaglieri *et al.*, arXiv:1707.04591 [hep-ph].

[6] There has been a huge amount of work on this subject; see, for example, D. Feldman, B. Kors and P. Nath, Phys. Rev. D **75**, 023503 (2007) [hep-ph/0610133]; D. Feldman, Z. Liu and P. Nath, Phys. Rev. D **75**, 115001 (2007) [hep-ph/0702123 [HEP-PH]].; M. Pospelov, A. Ritz and M. B. Voloshin, Phys. Lett. B **662**, 53 (2008) [arXiv:0711.4866 [hep-ph]]; M. Pospelov, Phys. Rev. D **80**, 095002 (2009) [arXiv:0811.1030 [hep-ph]]; H. Davoudiasl, H. S. Lee and W. J. Marciano, Phys. Rev. Lett. **109**, 031802 (2012) [arXiv:1205.2709 [hep-ph]] and Phys. Rev. D **85**, 115019 (2012) doi:10.1103/PhysRevD.85.115019 [arXiv:1203.2947 [hep-ph]]; R. Essig *et al.*, arXiv:1311.0029 [hep-ph]; E. Izaguirre, G. Krnjaic, P. Schuster and N. Toro, Phys. Rev. Lett. **115**, no. 25, 251301 (2015) [arXiv:1505.00011 [hep-ph]]; For a general overview and introduction to this framework, see D. Curtin, R. Essig, S. Gori and J. Shelton, JHEP **1502**, 157 (2015) [arXiv:1412.0018 [hep-ph]].

[7] B. Holdom, Phys. Lett. **166B**, 196 (1986) and Phys. Lett. B **178**, 65 (1986); K. R. Dienes, C. F. Kolda and J. March-Russell, Nucl. Phys. B **492**, 104 (1997) [hep-ph/9610479]; F. Del Aguila, Acta Phys. Polon. B **25**, 1317 (1994) [hep-ph/9404323]; K. S. Babu, C. F. Kolda and J. March-Russell, Phys. Rev. D **54**, 4635 (1996) [hep-ph/9603212]; T. G. Rizzo, Phys. Rev. D **59**, 015020 (1998) [hep-ph/9806397].

[8] For a recent overview of vector-like quarks and original references, see C. Y. Chen, S. Dawson and E. Furlan, Phys. Rev. D **96**, no. 1, 015006 (2017) [arXiv:1703.06134 [hep-ph]]; for a corresponding recent overview of vector-like leptons and original references, see Z. Poh and S. Raby, Phys. Rev. D **96**, no. 1, 015032 (2017) [arXiv:1705.07007 [hep-ph]]. For a general recent review of VLF, see V. Peralta, arXiv:1712.06193 [hep-ph].

[9] M. Aaboud *et al.* [ATLAS Collaboration]; arXiv:1808.02343 [hep-ex]; A. M. Sirunyan *et al.* [CMS Collaboration], arXiv:1805.04758 [hep-ex]; CMS Collaboration [CMS Collaboration], CMS-PAS-EXO-18-005.

[10] C. D. Carone, S. Chaurasia and T. V. B. Claringbold, arXiv:1807.05288 [hep-ph].

[11] N. Baltzell *et al.* [HPS Collaboration], Nucl. Instrum. Meth. A **859**, 69 (2017) [arXiv:1612.07821 [physics.ins-det]]; M. De Napoli [HPS Collaboration], EPJ Web Conf. **142**, 01011 (2017); P. H. Adrian *et al.* [HPS Collaboration], arXiv:1807.11530 [hep-ex].

[12] For more information about the LDMX experiment, see `https://confluence.slac.stanford.edu/display/MME/Light+Dark+Matter+Experiment`; T. Raubenheimer *et al.*, arXiv:1801.07867 [physics.acc-ph] and also T. Akesson *et al.* [LDMX Collaboration], arXiv:1808.05219 [hep-ex].

[13] T. G. Rizzo, JHEP **1807**, 118 (2018) [arXiv:1801.08525 [hep-ph]].

[14] T. G. Rizzo, JHEP **1810**, 069 (2018) [arXiv:1805.08150 [hep-ph]].

[15] M. S. Chanowitz and M. K. Gaillard, Nucl. Phys. B **261**, 379 (1985); B. W. Lee, C. Quigg and H. B. Thacker, Phys. Rev. D **16**, 1519 (1977); J. M. Cornwall, D. N. Levin and G. Tiktopoulos, Phys. Rev. D **10**, 1145 (1974) Erratum: [Phys. Rev. D **11**, 972 (1975)]; G. J. Gounaris, R. Kogerler and H. Neufeld, Phys. Rev. D **34**, 3257 (1986).

[16] For a recent review, see B. M. Roberts, V. A. Dzuba and V. V. Flambaum, Ann. Rev. Nucl. Part. Sci. **65**, 63 (2015) [arXiv:1412.6644 [physics.atom-ph]].

[17] J. Benesch *et al.* [MOLLER Collaboration], arXiv:1411.4088 [nucl-ex]; D. Androic *et al.* [Qweak Collaboration], Nature **557**, no. 7704, 207 (2018); K. Aulenbacher and A. Jankowiak, "Polarized Electrons and Positrons at the Mesa Accelerator,"

[18] M. Tanabashi *et al.* [ParticleDataGroup], Phys. Rev. D **98**, no. 3, 030001 (2018).

[19] J. P. Leveille, Nucl. Phys. B **137**, 63 (1978).

[20] See, for example, A. N. Khan and D. W. McKay, JHEP **1707**, 143 (2017) [arXiv:1704.06222 [hep-ph]].

[21] T. G. Rizzo, work in progress.

[22] We employ numerical estimates based on M. Czakon and A. Mitov, Comput. Phys. Commun. **185**, 2930 (2014) [arXiv:1112.5675 [hep-ph]].

[23] T. G. Rizzo, Phys. Rev. D **22**, 722 (1980); W. Y. Keung and W. J. Marciano, Phys. Rev. D **30**, 248 (1984).

[24] M. Bauer, P. Foldenauer and J. Jaeckel, JHEP **1807**, 094 (2018); [arXiv:1803.05466 [hep-ph]]. P. Ilten, Y. Soreq, M. Williams and W. Xue, JHEP **1806**, 004 (2018) [arXiv:1801.04847 [hep-ph]].

[25] M. Aaboud *et al.* [ATLAS Collaboration], JHEP **1711**, 195 (2017) [arXiv:1708.09266 [hep-ex]]; A. M. Sirunyan *et al.* [CMS Collaboration], Phys. Lett. B **778**, 263 (2018) [arXiv:1707.07274 [hep-ex]].

[26] LHC SUSY Cross Section Working Group, `https://twiki.cern.ch/twiki/bin/view/LHCPhysics/SUSYCrossSections`

[27] W. Beenakker, C. Borschensky, M. Kramer, A. Kulesza and E. Laenen, JHEP **1612**, 133 (2016) [arXiv:1607.07741 [hep-ph]].

[28] C. Alpigiani *et al.*, "A Letter of Intent for MATHUSLA: a dedicated displaced vertex detector above ATLAS or CMS.," CERN-LHCC-2018-025, LHCC-I-031.

[29] N. Arkani-Hamed and N. Weiner, JHEP **0812**, 104 (2008) [arXiv:0810.0714 [hep-ph]]; M. Baumgart, C. Cheung, J. T. Ruderman, L. T. Wang and I. Yavin, JHEP **0904**, 014 (2009) [arXiv:0901.0283 [hep-ph]]; A. Falkowski, J. T. Ruderman, T. Volansky and J. Zupan, Phys. Rev. Lett. **105**, 241801 (2010) [arXiv:1007.3496 [hep-ph]] and JHEP **1005**, 077 (2010) [arXiv:1002.2952 [hep-ph]]; C. Cheung, J. T. Ruderman, L. T. Wang and I. Yavin, JHEP **1004**, 116 (2010) [arXiv:0909.0290 [hep-ph]]; G. Barello, S. Chang, C. A. Newby and B. Ostdiek, Phys. Rev. D **95**, no. 5, 055007 (2017) [arXiv:1612.00026 [hep-ph]].

[30] J. de Favereau *et al.* [DELPHES 3 Collaboration], JHEP **1402**, 057 (2014) [arXiv:1307.6346 [hep-ex]].

[31] G. Aad *et al.* [ATLAS Collaboration], JHEP **1411**, 088 (2014) [arXiv:1409.0746 [hep-ex]]; G. Aad *et al.* [ATLAS Collaboration], JHEP **1602**, 062 (2016) [arXiv:1511.05542 [hep-ex]]; M. Del Gaudio [ATLAS Collaboration], PoS EPS **-HEP2017**, 690 (2018); ATLAS note ATLAS-CONF-2016-042; V. Khachatryan *et al.* [CMS Collaboration], Phys. Lett. B **752**, 146 (2016) [arXiv:1506.00424 [hep-ex]]; CMS Collaboration [CMS Collaboration], CMS-PAS-HIG-18-003.

[32] T. G. Rizzo, Phys. Rev. D **47**, 956 (1993) [hep-ph/9209207].